Journal of Environmental Radioactivity 290 (2025) 107810

Contents lists available at ScienceDirect

Journal of Environmental Radioactivity

journal homepage: www.elsevier.com/locate/jenr

Environmental and biological drivers of ^{137}Cs accumulation in freshwater fish across forested and downstream sites in Fukushima[☆]

Minato Kakuma [a,b,*], Toshihiro Wada [b], Masashi Murakami [c], Takahiro Tatsuno [d], Nobuyoshi Ishii [e], Natsuko I. Kobayashi [f], Takumi Kurosawa [g], Yo Sayama [a], Naoto Nihei [h], Nobuhito Ohte [a]

[a] Graduate School of Informatics, Kyoto University, Yoshida Hommachi, Sakyo-ku, Kyoto, 606-8501, Japan
[b] Institute of Environmental Radioactivity, Fukushima University, 1 Kanayagawa, Fukushima, 960-1296, Japan
[c] Graduate School of Science, Chiba University, 1-33 Yayoicho, Inage-ku, Chiba, 263-8522, Japan
[d] Research Faculty of Agriculture, Hokkaido University, Kita-9, Nishi-9, Kita-ku, Sapporo, Hokkaido, 060-8589, Japan
[e] Environmental Transfer Parameter Research Group, National Institutes for Quantum and Radiological Science and Technology, 4-9-1 Anagawa Inage-ku, Chiba, 263-8555, Japan
[f] Graduate School of Agricultural and Life Sciences, The University of Tokyo, 1-1-1 Yayoi, Bunkyo-ku, Tokyo, 113-8657, Japan
[g] Field Science Education and Research Center, Kyoto University, Maizuru, Kyoto, 625-0086, Japan
[h] Faculty of Food and Agricultural Science, Fukushima University, 1 Kanayagawa, Fukushima, 960-1296, Japan

ARTICLE INFO

Keywords:
Fukushima
Radiocesium
Freshwater fish
Forested streams
Stable isotope analysis
Trophic structure

ABSTRACT

To elucidate ecological factors governing ^{137}Cs accumulation in freshwater fish, we examined 10 species collected from forested headwater streams and downstream reaches of rivers flowing through the Fukushima evacuation zone between 2020 and 2022. By integrating land cover data with isotopic and body size metrics, our study clarifies mechanisms shaping radiocesium distribution across fish communities in post-accident environments. Individuals exceeding the Japanese regulatory limit of 100 Bq/kg-wet were found at all sites, and fish/water concentration ratios of ^{137}Cs varied widely, from 9.7×10 L/kg-wet in a sea-run masu salmon to 1.2×10^6 L/kg-wet in a Japanese dace. White-spotted charr and masu salmon, both typical stream-dwelling salmonids, exhibited significantly higher concentration ratios than the other species. Fish from areas with greater forest cover exhibited consistently elevated ^{137}Cs concentrations, indicating that forests serve as persistent sources of radiocesium to aquatic food webs more than a decade after the accident. Stable isotope analysis showed a significant positive association between terrestrial carbon contribution and ^{137}Cs concentration, demonstrating that individuals assimilating more terrestrial-derived resources tended to accumulate higher contamination. A positive relationship was also observed between relative body size and ^{137}Cs concentration, suggesting that growth-related traits influence accumulation. These results suggest that forest connectivity, dietary reliance on allochthonous resources, and individual growth characteristics collectively influence the accumulation of ^{137}Cs in freshwater fish. The approach and findings provide quantitative evidence for species- and site-specific processes underlying long-term radiocesium dynamics in forested river networks, informing risk assessment and fisheries management in radiologically impacted landscapes.

☆ This work was supported by the Japan Society for the Promotion of Science (JSPS) through a Grant -in-Aid for JSPS Fellows (JP22KJ1930) and a JSPS KAKENHI Grant (JP20H00435), as well as by the Fukushima Institute for Research, Education and Innovation (F-REI) through a commissioned research fund (JPFR25050501). The authors thank Honoka Kurosawa and Hiromichi Waki for their valuable assistance with sample processing and analysis.

* Corresponding author at: Institute of Environmental Radioactivity, Fukushima University, 1 Kanayagawa, Fukushima, 960-1296, Japan.
E-mail addresses: m-kakuma@ier.fukushima-u.ac.jp (M. Kakuma), t-wada@ipc.fukushima-u.ac.jp (T. Wada), muramasa@faculty.chiba-u.jp (M. Murakami), t.tatsuno@agr.hokudai.ac.jp (T. Tatsuno), ishii.nobuyoshi@qst.go.jp (N. Ishii), anikoba@g.ecc.u-tokyo.ac.jp (N.I. Kobayashi), kurosawa.takumi.48x@st.kyoto-u.ac.jp (T. Kurosawa), sayama.yo.67c@st.kyoto-u.ac.jp (Y. Sayama), nihei@agri.fukushima-u.ac.jp (N. Nihei), nobu@i.kyoto-u.ac.jp (N. Ohte).

https://doi.org/10.1016/j.jenvrad.2025.107810
Received 10 July 2025; Received in revised form 6 September 2025; Accepted 8 September 2025

1. Introduction

The Fukushima Daiichi Nuclear Power Plant (FDNPP) accident in 2011 released large quantities of radioactive cesium isotopes (^{134}Cs and ^{137}Cs) into the environment, leading to extensive contamination of inland aquatic ecosystems. Due to its longer half-life (30.2 years) compared to ^{134}Cs (2.06 years), ^{137}Cs persists in the environment and has become the primary focus of long-term environmental monitoring. Given the long half-life of ^{137}Cs, forested and aquatic habitats in the affected region remain contaminated many years after the accident (Hayashi, 2016), posing continued risks, especially in inland fisheries and areas designated as "Difficult-to-Return Zones" (Wada et al., 2022). After deposition onto terrestrial landscapes, ^{137}Cs is primarily transported into river systems via runoff and suspended sediments (Ueda et al., 2013; Ohte et al., 2016). This process leads to long-term contamination of aquatic habitats and biota, including freshwater fish, which are both ecologically and commercially important. Therefore, understanding the ecological dynamics of ^{137}Cs — particularly its accumulation and transfer within aquatic food webs, as well as its input from surrounding environments — is essential for effective remediation and long-term environmental management.

Although over a decade has passed since the accident, ^{137}Cs contamination in freshwater fish remains a serious concern. Compared to marine species, riverine fish often exhibit higher ^{137}Cs concentrations (Wada et al., 2019). In marine systems, radiocesium concentrations in seawater rapidly decreased due to diffusion after the FDNPP accident (Aoyama et al., 2019), and direct uptake from water or prey has become less influential for fish. Furthermore, the much greater potassium (K^+) concentrations in seawater reduce ^{137}Cs uptake through ionic competition (Rowan and Rasmussen, 1994; Wada et al., 2023). In contrast, in freshwater systems, radiocesium incorporated into forest and aquatic ecosystems is retained and recycled, thereby continuing to enter food webs and sustain contamination of fish through dietary pathways (Haque et al., 2017; Wada et al., 2019). Forests, which cover much of the upstream landscape in the affected region, have been identified as long-term sources of ^{137}Cs to river ecosystems through pathways such as leaf litter, soil erosion, and leaching (Kurikami et al., 2019; Sakai et al., 2021). The gradual decline of dissolved ^{137}Cs concentrations in rivers further suggests that these forest-derived inputs may continue to sustain contamination in aquatic food webs for decades (Nakanishi and Sakuma, 2019). To understand the long-term dynamics of freshwater contamination, it is essential not only to monitor ^{137}Cs concentrations in fish but also to quantify the pathways and magnitudes of ^{137}Cs transfer to aquatic organisms (Tsuji et al., 2014b; Wada et al., 2016, 2022). Clarifying these transfer mechanisms is critical for developing practical risk assessments and informing future remediation strategies.

Factors influencing ^{137}Cs accumulation in fish include diet, life history traits, and environmental conditions (Wada et al., 2016, 2024; Ishii et al., 2020). Dietary uptake is considered the dominant pathway, rather than uptake from water (Yamamoto et al., 2015; Matsuda et al., 2020; Wada et al., 2023). Comparative studies between marine and freshwater environments and between lakes and rivers have aimed to clarify how environmental conditions and habitat types influence ^{137}Cs accumulation patterns in fish (Wada et al., 2019; Ishii et al., 2020). Recent studies have applied stable isotope analyses of carbon and nitrogen to examine the relationship between food web structure and ^{137}Cs transfer (Ishii et al., 2023; Wada et al., 2024). However, little research has examined how transitions in surrounding environments — from forested upstream reaches to inhabited downstream areas — affect ^{137}Cs transfer to fish inhabiting those ecotones. Moreover, while the "size effect" — wherein larger fish exhibit higher ^{137}Cs concentrations — is well documented (Koulikov and Ryabov, 1992; Wada et al., 2019; Ishii et al., 2020), its underlying causes remain unclear in riverine species, particularly given the lack of consistent correlation between trophic position and ^{137}Cs levels (Ishii et al., 2020). To better understand this phenomenon, it is essential to consider multiple explanatory variables that capture different biological aspects. Body size metrics (e.g., length and weight) represent physical growth, trophic position reflects feeding relationships within the food web, and condition factor serves as an indicator of the nutritional status of freshwater fish.

This study aimed to characterize ^{137}Cs accumulation in freshwater fish from rivers affected by the FDNPP accident approximately 10 years post-disaster. Specifically, we evaluated how site-level contamination, forest cover, dietary indicators derived from stable isotope analysis, and individual morphological traits influenced ^{137}Cs concentrations in 10 fish species collected from multiple rivers near the FDNPP between 2020 and 2022. Sampling sites were selected to encompass a range of forest cover and contamination levels, from upstream forested streams to downstream areas. We included fish species with diverse feeding habits and migratory behaviors to assess the combined effects of diet, life history traits, and environmental conditions. Stable isotope analysis was used to estimate the contributions of terrestrial carbon and trophic position. These data allowed us to evaluate the pathways of ^{137}Cs transfer to individual fish via the food web and provide new insights into freshwater fish across contaminated river systems.

2. Materials and methods

2.1. Study site

This study was conducted in three rivers in Fukushima Prefecture (Fig. 1). The Ukedo and Takase Rivers are located to the north of the FDNPP, and the Kuma River is located to the south. The Takase River branches off from the Ukedo River 1.6 km upstream from its mouth. These three rivers flow through the "Difficult-to-Return Zone" established after the nuclear power plant accident (Fukushima Prefecture, 2024). The survey was conducted at three locations along the upper and lower reaches of each river: U1, U2, and U3 for the Ukedo River; T1, T2, and T3 for the Takase River; and K1, K2, and K3 for the Kuma River (Fig. 1; Table 1). All sample collection was carried out within a 500 m area along the river channel and a 50 m area from the center of the river (Fig. 1c).

As an indicator of the differences in the surrounding environment in the longitudinal direction of the river, percentages of forests (deciduous broad-leaved forests, deciduous needle-leaved forests, evergreen broad-leaved forests, and evergreen needle-leaved forests) within the sample collection areas were calculated from the high-resolution land use and land cover map data (Japan Aerospace Exploration Agency, 2023). Most of the target area is covered by forests at the uppermost study site of the Ukedo and Kuma Rivers (Table 1). Average ^{137}Cs depositions, used as an indicator of terrestrial radiocesium contamination, were calculated by decay-correcting the airborne monitoring data (Japan Atomic Energy Agency, 2024) for each year to the sample collection date (Table S1). ^{137}Cs contamination levels at the upstream study sites are high for the Ukedo and Takase Rivers (Fig. 1; Table S1). In contrast, the contamination levels at the downstream study sites are high for the Kuma River. The software QGIS version 3.34 (QGIS Development Team, 2024) was used to calculate the percentages of forests and the average ^{137}Cs depositions.

2.2. Sample collection

All samples were collected between October 2020 and October 2022. Freshwater fish were collected both for ^{137}Cs concentration measurements and stable isotope analysis. River water and riverbed sediments were sampled for ^{137}Cs concentration measurements. Periphyton, terrestrial plants, and aquatic insects were collected for stable isotope analysis.

Freshwater fish were collected at all sites in October of each year using an electrofisher (LR-20B; Smith-Root Inc.). However, no collection

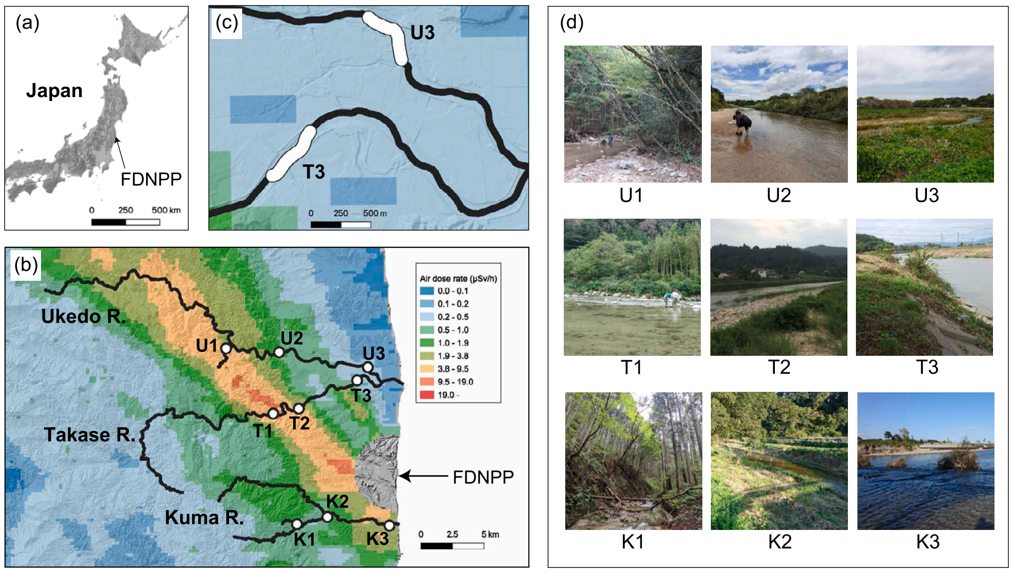

Fig. 1. The study area overview. The maps are based on the shaded-relief map of the Geospatial Information Authority of Japan. (a) The Fukushima Daiichi Nuclear Power Plant (FDNPP) location. (b) Locations of the Ukedo River, Takase River, Kuma River, and the FDNPP in Fukushima Prefecture and the study sites. The air dose rates at a height of 1 m are based on data from the Nuclear Regulation Authority's 15th airborne monitoring in 2020. (c) The white-painted areas on the map show an example of sample collection target areas. (d) Photographs of the study sites.

Table 1
Summary of sampling locations and the percentages of forests within the sample collection areas calculated from the high-resolution land use and land cover map data.

River	Site	Latitude (°N)	Longitude (°E)	Altitude (m)	Percentage of forests in land use
Ukedo R.	U1	37.5108	140.8824	139	99.99
	U2	37.5077	140.9300	29	16.85
	U3	37.4964	141.0094	2	2.05
Takase R.	T1	37.4643	140.9240	45	47.70
	T2	37.4676	140.9470	24	10.02
	T3	37.4871	140.9997	6	2.33
Kuma R.	K1	37.3859	140.9441	110	99.94
	K2	37.3907	140.9715	43	19.19
	K3	37.3841	141.0271	5	19.21

Table 2
Summary of collected fish samples. Numbers in parentheses indicate sea-run individuals. The a and b values are coefficients in the standard allometric equation $W = aL^b$, where W is fresh weight (g) and L is total length (cm).

Species	Scientific name	*N*									Factors in the standard allometric equations	
		U1	U2	U3	T1	T2	T3	K1	K2	K3	a	b
White-spotted charr	*Salvelinus leucomaenis*	17					1				1.03×10^{-2}	3.03
Masu salmon	*Oncorhynchus masou*	38	5 (1)	1	12 (1)		2	40			3.70×10^{-2}	2.59
Japanese dace	*Pseudaspius hakonensis*		12	20	30	25	15		20	16	4.59×10^{-3}	3.25
Japanese seabass	*Lateolabrax japonicus*			5							1.07×10^{-3}	3.83
Flathead grey mullet	*Mugil cephalus*			8						7	5.97×10^{-3}	3.19
Japanese catfish	*Silurus asotus*		4	3			1				2.60×10^{-2}	2.67
Common carp	*Cyprinus carpio*			3						7	2.93×10^{-2}	2.82
Japanese eel	*Anguilla japonica*		7	36	1		4			30	1.06×10^{-4}	3.68
Ayu	*Plecoglossus altivelis*		18	30	30	30	30			20	6.40×10^{-3}	3.05
Pale chub	*Opsariichthys platypus*			18		11	21		2	16	2.82×10^{-3}	3.42

was conducted at sites U2 and K2 in 2021. A total of 596 individuals representing 10 species were collected (Table 2). The species included white-spotted charr, masu salmon, Japanese dace, Japanese seabass, flathead grey mullet, Japanese catfish, common carp, Japanese eel, ayu, and pale chub.

On the same day as the fish sampling, river water and riverbed sediments (upper 3 cm depth) were collected under base-flow conditions. The river water was collected in plastic containers, each approximately 20 L in volume. Sediment samples were collected three times using a scoop.

Periphyton, which represents river-derived food resources, was collected by brushing the surface of rocks picked up from the riverbed and rinsing them with distilled water. As terrestrial plant samples representing land-derived food resources, fresh leaves of major tree species were collected from the surrounding land in the target area.

Aquatic insects were collected as isotopic baselines for estimating the trophic positions of freshwater fish based on nitrogen stable isotope ratios. Unlike periphyton, which is known to exhibit substantial isotopic variability due to its short lifespan and intense sensitivity to fluctuations in the δ^{15}N of dissolved inorganic nitrogen, aquatic insects provide a more temporally integrated baseline of assimilated riverine resources (Post, 2002). They were collected by disturbing the riverbed upstream of a D-frame net (mesh size: 250 μm) placed on the bottom.

2.3. Sample processing

Fish samples were rinsed with water, and their total length and body weight were measured. For masu salmon, individuals with total lengths up to 30 cm were classified as fluvial (residential) type, while those exceeding 35 cm were considered sea-run type. No individuals with intermediate sizes (30–35 cm) were observed, as the two types were distinct in body size. Following the Fukushima Prefectural monitoring protocol (Wada et al., 2016), ^{137}Cs concentrations were determined using either muscle tissue alone or bodies excluding the head and internal organs. For groups in which individuals often exceeded 200 g in body weight (sea-run type of masu salmon, Japanese catfish, common carp, and Japanese eel), only muscle tissue was analyzed. For the other groups (white-spotted charr, fluvial type of masu salmon, Japanese dace, Japanese seabass, flathead grey mullet, ayu, and pale chub), bodies excluding the head and internal organs were analyzed. Previous analyses (Wada et al., 2024) showed that ^{137}Cs concentrations in masu salmon bodies excluding the head and internal organs were approximately 89% of those in muscle tissue, indicating that the two measurement methods can be validly compared. The samples for ^{137}Cs analysis were homogenized and packed into plastic containers (U8; diameter: 55 mm, height: 64 mm). After measuring the wet weight, the samples were dried using a freeze dryer (FRD-51; Iwaki Glass Co., Ltd.), and the dry weight was subsequently measured.

A portion of muscle tissue was dissected from each fish for stable isotope analysis. These tissues were dried at 60 °C for 2–3 days using an electric constant-temperature dryer (DK340S; Yamato Scientific Co., Ltd.) and ground into powder. To minimize the influence of lipid content on δ^{13}C values, the powdered samples were lipid-extracted with a 2:1 chloroform–methanol solution for 24 h (Post et al., 2007).

River water samples were first filtered to remove particulate ^{137}Cs using either glass fiber filters (GF/F; Whatman) or nonwoven fabric cartridge filters (RP13-011; Japan Vilene Co., Ltd.; Tsuji et al., 2014a). Dissolved ^{137}Cs was collected using nonwoven fabric cartridge filters impregnated with potassium zinc ferrocyanide (CS-13ZN; Japan Vilene Co., Ltd.). These filters, which adsorbed dissolved ^{137}Cs, were dried and used directly for ^{137}Cs concentration measurements (Yasutaka et al., 2015). Riverbed sediment samples were dried at 80 °C for 2–3 days in the dryer, sieved through a 2 mm mesh, and packed into plastic containers (U9; diameter: 55 mm, height: 38 mm) for ^{137}Cs analysis after weighing.

Periphyton samples were collected via vacuum filtration through the glass fiber filters, using a dry vacuum pump (Rocker 300; Sibata Scientific Technology Ltd.) and a filter unit (300–4100; Thermo Fisher Scientific Inc.). The filters were exposed to hydrochloric acid to eliminate the influence of carbonate on δ^{13}C values and then rinsed with distilled water. The filters were dried at 60 °C for 2–3 days in the dryer, and the retained material was scraped off for analysis. Terrestrial plant samples were dried at 60 °C for 2–3 days and powdered using a grinding mill (IFM-C20G; Iwatani Corp.) for stable isotope analysis.

Aquatic insect samples were identified at the lowest possible taxonomic level in the laboratory. The samples were homogenized after drying at 60 °C for 2–3 days in the dryer. Whole-body samples, including gut contents, were used for stable isotope analysis.

2.4. ^{137}Cs concentration measurement

The activity concentrations of ^{137}Cs in freshwater fish, cartridge filters for collecting dissolved radiocesium from river water, and riverbed sediment samples were determined using high-purity germanium (HPGe) semiconductor detectors.

Fish samples collected from 2020 to 2022 and river water samples collected from 2021 to 2022 were analyzed using HPGe detectors (GC3018, GC4018, GC4020; Canberra) calibrated with volume standard sources (MX033U8PP; The Japan Radioisotope Association). Depending on the gamma emission intensity of each sample, the counting time for these measurements ranged from 155 to 240,000 s for fish and from 35,000 to 140,000 s for river water. Additional measurements were performed before freeze-drying for a subset of fish samples to confirm that ^{137}Cs activity remained consistent before and after the drying process.

Riverbed sediment samples collected in 2020–2022 and river water samples collected in 2020 were analyzed using HPGe detectors (GEM and GMX types; Seiko EG&G) calibrated with standard solutions. The standard solutions were prepared from pre-measured ^{137}Cs stock solutions and were used with decay correction applied based on the half-life of ^{137}Cs. The counting time was set at 3600 s for sediment samples and ranged from 3600 to 5400 s for river water.

Most samples were measured with a counting error of less than 10%. All activity concentrations were corrected for radioactive decay to the date of sample collection. The activity concentrations initially obtained for fish samples on a dry-weight basis were converted to a wet-weight basis using measured moisture content. Sediment concentrations were reported in dry weight, while dissolved ^{137}Cs concentrations in river water were expressed per unit volume of filtered water.

2.5. Stable isotope analysis

Approximately 1.0 mg of each sample, prepared for isotopic analysis, was accurately weighed and encapsulated in tin capsules.

The isotopic measurements were conducted using an integrated system comprising a mass spectrometer (Delta V Advantage; Thermo Fisher Scientific Inc.) connected to an elemental analyzer (Flash 2000; Thermo Fisher Scientific Inc.) via an interface unit (Conflo IV; Thermo Fisher Scientific Inc.). The isotopic ratios were expressed in delta notation as follows:

$$\delta X = (R_{sample}/R_{standard} - 1) \quad (1)$$

where X represents either ^{13}C or ^{15}N, and R denotes the ratio of $^{13}C/^{12}C$ or $^{15}N/^{14}N$. The $R_{standard}$ values were referenced against the Vienna Pee Dee Belemnite (VPDB) standard for carbon and atmospheric nitrogen for nitrogen measurements. Working standards (alanine, proline, and tyrosine; JCAC-01-0011, JCAC-02-0011, JCAC-03-0011; Japan Chemical Analysis Center) with known isotopic values were analyzed to ensure analytical precision and accuracy.

2.6. Data analysis

All statistical analyses were performed using R software version 4.3.3 (R. Core Team, 2024).

A linear regression model was applied for fish samples to examine the relationship between ^{137}Cs radioactivity in the container before and after freeze-drying. Then, to assess the potential influence of sampling date on the ^{137}Cs concentrations in fish samples collected from 2020 to 2022, generalized linear mixed models (GLMMs) were constructed using the `lmer()` function from the R package `lme4` version 1.1.35.1 (Bates et al., 2015). Sampling location and fish species were included as random effects. Two models were compared: one incorporating sampling date as a fixed effect, and a reduced model excluding it (hereafter referred to as the "null model"). The comparison was based on the Akaike Information Criterion (AIC).

Statistical comparisons of ^{137}Cs concentrations in fish among sampling sites were performed using the Steel–Dwass test implemented via the `pSDCFlig()` function in the R package `NSM3` version 1.18 (Schneider et al., 2023). To evaluate the transfer of ^{137}Cs from the surrounding ecosystem to each fish species, the concentration ratio (L/kg-wet) was calculated using the following equation:

$$\text{Concentration ratio} = {}^{137}\text{Cs}_{\text{fish}} / {}^{137}\text{Cs}_{\text{water}} \tag{2}$$

where $^{137}\text{Cs}_{\text{fish}}$ and $^{137}\text{Cs}_{\text{water}}$ represent the ^{137}Cs concentrations in fish (Bq/kg-wet) and the dissolved ^{137}Cs concentrations in river water (Bq/L), respectively. Statistical comparisons of concentration ratio among fish species were also conducted using the Steel–Dwass test.

To estimate the proportional contributions of carbon sources to freshwater fish, we constructed Bayesian stable isotope mixing models using the R package `MixSIAR` version 3.1.12 (Stock et al., 2018). Model fitting was performed via Markov Chain Monte Carlo (MCMC) sampling using the R package `rjags` version 4.16 (Plummer, 2024), which interfaces with the JAGS engine. The models were based on the δ^{13}C values of fish and those of their potential dietary sources. Site-specific means and standard deviations of source isotope values were used as inputs (Table S2). As sources, we used periphyton (representing aquatic primary production) and leaves of terrestrial plants (representing allochthonous input), both of which were collected from the same sites as the fish. The models allowed us to evaluate whether fish carbon sources originated from aquatic or terrestrial ecosystems. A carbon trophic enrichment factor of 1.93‰ was applied to fish muscle tissue for trophic fractionation. This value was adopted by Ishii et al. (2023), the trophic enrichment factor based on the method of Caut et al. (2009) and empirical data on fish diet δ^{13}C. The values of the fish δ^{13}C were adjusted using this trophic enrichment factor before model fitting to account for isotopic fractionation during assimilation. The JAGS model was generated using the `write_JAGS_model()` function, including residual and process error terms. The model was run using three MCMC chains with 100,000 iterations each, a burn-in of 50,000, and a thinning interval of 50. Model convergence was assessed using the Gelman–Rubin and Geweke diagnostics. The contribution of terrestrial plant carbon for each fish was summarized as the posterior mean of the estimated proportions.

The trophic position of fish was calculated based on the difference in δ^{15}N values between predators and their prey, using the following equation:

$$\text{Trophic position} = 2 + (\delta^{15}\text{N}_{\text{fish}} - \delta^{15}\text{N}_{\text{reference}})/3.4 \tag{3}$$

where $\delta^{15}\text{N}_{\text{fish}}$ is the nitrogen stable isotope value of the fish, and $\delta^{15}\text{N}_{\text{reference}}$ is that of the reference sample. The reference sample consisted of aquatic consumer taxa serving as the isotopic baseline of the aquatic ecosystem (Post, 2002; Table S2), primarily including Trichoptera and Plecoptera. In addition, insects belonging to Odonata and Megaloptera, whose δ^{15}N values were comparable to those of Trichoptera and Plecoptera, were also included as reference organisms in the trophic position calculation. A nitrogen trophic enrichment factor of 3.4‰ was used (Post, 2002).

To evaluate relative body size within species, fish total length data were standardized to have a mean of 0 and a standard deviation of 1 for each species. When standardizing, data on sea-run type of masu salmon and fluvial masu salmon were separated. The condition factor, an indicator of the nutritional status of freshwater fish, was calculated using the following equation:

$$\text{Condition factor} = \frac{W}{aL^b} \tag{4}$$

where W is the fresh body weight (g) and L is the fish's total length (cm). The parameters a and b are coefficients of the standard allometric equation:

$$W = aL^b. \tag{5}$$

These coefficients were empirically estimated for each species based on the data collected in this study (Table 2).

To assess the factors influencing ^{137}Cs concentrations in fish, we fitted generalized linear models (GLMs) with a Gaussian error distribution using the `glm()` function in R. The response variable was log-transformed wet weight-based ^{137}Cs concentration. The full model included the following explanatory variables: percentage of forests in land use within the sample collection areas, contribution of terrestrial plant carbon, standardized total length, condition factor, trophic position, log-transformed ^{137}Cs concentration in sediment, log-transformed dissolved ^{137}Cs concentration in water, and log-transformed average ^{137}Cs deposition within the sample collection areas. To check for multicollinearity among explanatory variables, we calculated the variance inflation factor (VIF) using the `vif()` function from the R package `car` version 3.1.2 (Fox and Weisberg, 2019). All VIFs were below 3, a conservative threshold adopted in Zuur et al. (2010). Model selection was conducted using the `dredge()` function from the R package `MuMIn` version 1.47.5 (Bartoń, 2023). All possible subsets of the full model were compared based on AIC, and the model with the lowest AIC was selected as the best-supported model. This approach allowed us to identify the most parsimonious combination of ecological and environmental predictors of ^{137}Cs concentrations in freshwater fish. To evaluate the relative importance of each explanatory variable included in the best-supported model, we compared the AIC of reduced models in which a single variable was dropped from the best-supported model. The difference in AIC between the original best-supported model and each reduced model (ΔAIC) was used as a metric of explanatory power for that variable. A larger ΔAIC indicates a greater decrease in model performance when omitted, suggesting that the variable has a relatively higher explanatory value within the model context.

3. Results

First, we evaluated the effect of freeze-drying on ^{137}Cs concentrations in fish samples. As shown in Fig. S1, radioactivity measured before and after freeze-drying were strongly correlated, with a regression equation of $y = 0.967x - 0.0398$ ($R^2 = 1.00$, $p < 0.001$), where x and y represent ^{137}Cs radioactivity in fish samples before and after freeze-drying (Bq). Given the nearly perfect fit, this result supports the validity of estimating wet weight-based ^{137}Cs concentrations from dry weight values using the sample-specific wet-to-dry weight ratio, even for samples measured only after freeze-drying.

Temporal variation in ^{137}Cs concentrations in fish samples collected from 2020 to 2022 was not supported by model comparison. The null model, which excluded the sampling date, showed a substantially better fit (ΔAIC = 20.1) than the model, including it as a fixed effect. Thus, no significant temporal trend was assumed in subsequent analyses.

3.1. Variation in ^{137}Cs concentrations among sites and species

596 individuals representing 10 fish species were analyzed for ^{137}Cs concentrations, ranging from a minimum of 3.6 Bq/kg-wet to a maximum of 2.1×10^4 Bq/kg-wet. At all study sites, we detected individual fish whose ^{137}Cs concentrations exceeded the Japanese regulatory limit of 100 Bq/kg-wet (Fig. 2). In the Takase River, no apparent differences in ^{137}Cs concentrations were observed among the sampling sites. In contrast, in both the Ukedo and Kuma Rivers, fish collected from different sites within the same river exhibited statistically significant differences in ^{137}Cs concentrations (Steel–Dwass test, $p < 0.05$). In both rivers, fish collected from the uppermost sites — characterized by high forest cover — showed the highest ^{137}Cs concentrations. In the Ukedo River, ^{137}Cs concentrations decreased in the order of upstream > midstream > downstream. In contrast, in the Kuma River, concentrations were higher at the downstream site, closer to the FDNPP, than at the midstream site.

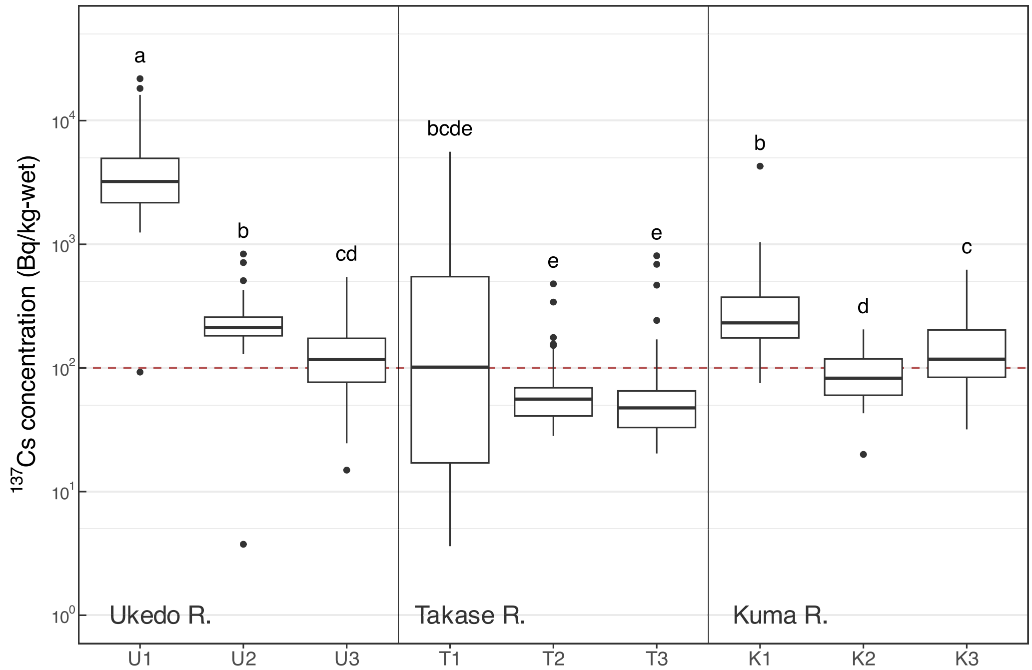

Fig. 2. Boxplots showing ^{137}Cs concentrations in fish collected from each study site. The horizontal line within each box represents the median, and the box spans the interquartile range (25th to 75th percentiles). Whiskers indicate the 5th and 95th percentiles, and points represent outliers. Different letters above boxes denote significant site differences ($p < 0.05$). The horizontal dashed line represents the Japanese regulatory limit (100 Bq/kg-wet).

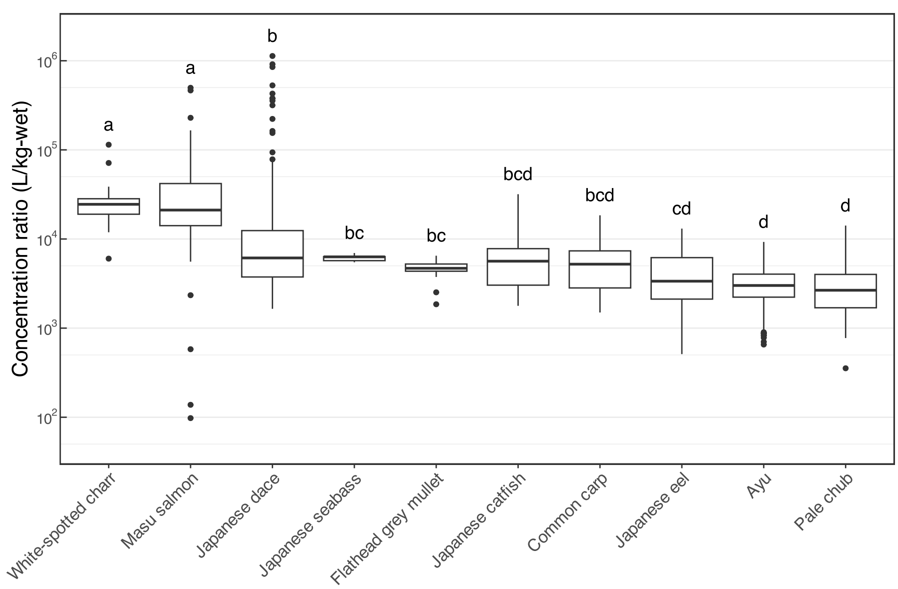

Fig. 3. Boxplots showing ^{137}Cs concentration ratios in fish, grouped by species. Concentration ratio was calculated as the ratio of ^{137}Cs concentration in fish (Bq/kg-wet) to that in river water (Bq/L), with units of L/kg-wet. The horizontal line within each box represents the median, and the box spans the interquartile range (25th to 75th percentiles). Whiskers indicate the 5th and 95th percentiles, and points represent outliers. Different letters above boxes denote significant differences among species ($p < 0.05$).

The fish/water concentration ratios of ^{137}Cs ranged from 9.7×10 to 1.2×10^6 L/kg-wet across all individuals. The highest concentration ratio was observed in a Japanese dace, whereas the lowest was found in a sea-run type of masu salmon (Fig. 3). Among the species examined, the white-spotted charr and masu salmon, both typical stream-dwelling salmonids, exhibited significantly higher concentration ratios than the other species (Steel–Dwass test, $p < 0.05$). For species such as masu salmon and Japanese dace, within-species variations in concentration ratios reached three to four orders of magnitude.

Two individuals of sea-run type masu salmon collected in the Ukedo and Takase Rivers exhibited ^{137}Cs concentrations of approximately 4 Bq/kg-wet, the lowest values recorded among all fish individuals in this study. These values were markedly lower than those observed in fluvial type individuals of the same species collected at the same sites, which ranged from 1.5×10^2 to 2.9×10^2 Bq/kg-wet at the midstream site U2 and from 4.0×10^2 to 2.2×10^3 Bq/kg-wet at the upstream site T1 (Fig. 4a). Other fish species collected at these sites showed ^{137}Cs concentrations ranging from 1.3×10^2 to 8.3×10^2 Bq/kg-wet at site

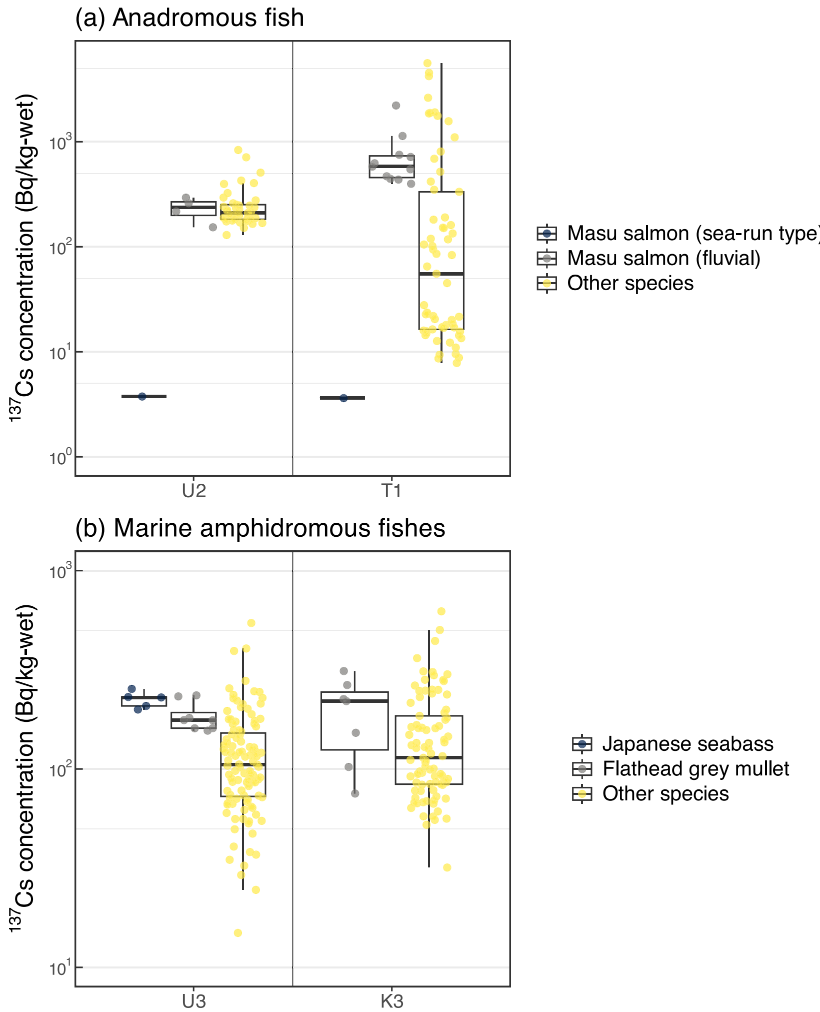

Fig. 4. Boxplots overlaid with jittered individual data points showing ^{137}Cs concentrations in fish. (a) Fish collected at sites U2 and T1, where the sea-run type of anadromous masu salmon was present. Masu salmon (sea-run type), masu salmon (fluvial), and all other species are shown separately. (b) Fish collected at sites U3 and K3, where marine amphidromous species were present. Japanese seabass, flathead grey mullet, and all other species are shown separately. The horizontal line within each box indicates the median, the box spans the interquartile range (25th to 75th percentiles), and the whiskers extend to the 5th and 95th percentiles.

U2 and from 7.8 to 5.6×10^3 Bq/kg-wet at site T1. In contrast, marine amphidromous fish species, namely Japanese seabass and flathead grey mullet, exhibited ^{137}Cs concentrations comparable to or higher than those of other freshwater species collected at the same downstream sites (Fig. 4b). At site U3, Japanese seabass and flathead grey mullet showed concentrations ranging from 2.0×10^2 to 2.5×10^2 Bq/kg-wet and 1.6×10^2 to 2.4×10^2 Bq/kg-wet, respectively, whereas other fish species ranged from 1.5×10 to 5.4×10^2 Bq/kg-wet. At site K3, flathead grey mullet exhibited 7.5×10 to 3.1×10^2 Bq/kg-wet concentrations, while other species ranged from 3.2×10 to 6.2×10^2 Bq/kg-wet.

3.2. *Factors influencing ^{137}Cs concentrations in fish*

Model selection based on AIC revealed that the best-supported model included eight explanatory variables: percentage of forests in land use, contribution of terrestrial plant carbon, standardized total length, condition factor, trophic position, and log-transformed values of sediment ^{137}Cs concentration, dissolved ^{137}Cs concentration in water, and average ^{137}Cs deposition at the site (Table 3). The top three models differed by less than 2 AIC units, indicating that they were almost statistically indistinguishable and provided similarly good fits to the data.

Table 3
Top-ranked generalized linear models selected based on AIC. The response variable was log-transformed wet weight-based ^{137}Cs concentration in fish. Explanatory variables are abbreviated as follows: `Forst`, percentage of forests in land use; `Plant`, contribution of terrestrial plant carbon; `Lngth`, standardized total length; K, condition factor; TP, trophic position; `lgSdm`, log-transformed sediment ^{137}Cs concentration; `lgWtr`, log-transformed dissolved ^{137}Cs concentration in water; `lgDps`, log-transformed average ^{137}Cs deposition at the site. ΔAIC indicates the difference in AIC from the best-supported model (top row). Only models with $\Delta AIC < 2$ are shown.

Model	AIC	ΔAIC
Forst + Plant + Lngth + lgSdm + lgWtr + K + TP + lgDps	558.0	0.0
Forst + Plant + Lngth + lgSdm + lgWtr + K + TP	558.5	0.6
Forst + Plant + Lngth + lgSdm + lgWtr + K + lgDps	558.8	0.8

Parameter estimates for this best-supported model are shown in Table 4. All predictors except for the trophic position and ^{137}Cs deposition had statistically significant effects ($p < 0.001$), and all VIF values were below 3, indicating no substantial multicollinearity among variables. The percentage of forests showed the greatest explanatory importance among the explanatory variables, as indicated by the largest

Table 4
Parameter estimates and relative importance of explanatory variables in the best-supported generalized linear model explaining log-transformed wet weight-based ^{137}Cs concentrations in fish (Table 3). VIF refers to the variance inflation factor used to assess multicollinearity. ΔAIC indicates the change in AIC when each variable is individually removed from the best-supported model, with larger values indicating greater explanatory importance. Estimates are presented with 95% confidence intervals (CIs).

Parameter	VIF	Estimate	CI	*P*	ΔAIC
(Intercept)		0.92	(0.18, 1.65)		
Percentage of forests in land use	1.7	0.76	(0.65, 0.88)	< 0.001	146.3
Contribution of terrestrial plant carbon	1.1	0.96	(0.72, 1.21)	< 0.001	55.5
Standardized total length	1.1	0.12	(0.09, 0.15)	< 0.001	51.2
^{137}Cs concentration in sediment	2.4	0.52	(0.38, 0.66)	< 0.001	49.0
Dissolved ^{137}Cs concentration in water	2.3	0.38	(0.26, 0.50)	< 0.001	39.0
Condition factor	1.1	−0.33	(−0.52, −0.15)	< 0.001	10.3
Trophic position	1.3	−0.07	(−0.15, 0.01)	0.095	0.8
^{137}Cs deposition	1.5	0.05	(−0.01, 0.11)	0.113	0.6

ΔAIC value (146.3) when excluded from the model. This was followed by the contribution of terrestrial plant carbon (55.5), standardized total length (51.2), and sediment ^{137}Cs concentration (49.0), suggesting that both landscape-level and physiological factors contributed to variation in fish ^{137}Cs contamination. Fig. 5 illustrates the relationships between each predictor and the log-transformed ^{137}Cs concentration in fish based on model predictions.

4. Discussion

4.1. Environmental factors affecting ^{137}Cs accumulation

At all sampling sites in this study, freshwater fish exceeding the Japanese regulatory limit of 100 Bq/kg-wet for ^{137}Cs were detected (Fig. 2). Additionally, including the sampling date as a predictor variable did not improve the statistical models of ^{137}Cs concentration in fish, suggesting that the observed radiocesium contamination has entered a phase of negligible decline. This trend implies persistent contamination in rivers draining the “Difficult-to-Return Zone”, in contrast to earlier phases reported in previous studies, such as Wada et al. (2016), where more rapid decreases in radiocesium concentrations were observed — likely driven by the initial washout of dissolved ^{137}Cs shortly after the accident.

Fish are generally capable of moving within river systems, including between upstream and downstream reaches, despite upstream movement being sometimes restricted by physical barriers, such as weirs and waterfalls. Nevertheless, our results showed significant differences in ^{137}Cs concentrations among sampling sites within the same river, even when no physical barriers were present (Ukedo and Kuma Rivers; Fig. 2). While both terrestrial deposition and concentrations in river water of ^{137}Cs exhibited apparent spatial heterogeneity (Table S1), their explanatory power for fish ^{137}Cs concentrations was limited. According to the model selection results, the top three models differed by less than two AIC units (Table 3), suggesting that the inclusion or exclusion of variables such as terrestrial ^{137}Cs deposition did not substantially affect model fit. Accordingly, these predictors appear to be of relatively low importance for explaining variation in fish contamination, consistent with their low ΔAIC values in the variable importance analysis (Table 4). River water ^{137}Cs concentrations had moderate explanatory power but were not among the top-ranked predictors in the models (Table 4; Fig. 5). Crucially, however, fish/prey concentration ratios remain more stable across contamination gradients (Haque et al., 2017), which was also supported by the present results showing stronger explanatory power of ^{137}Cs concentrations in riverbed sediments for the fish ^{137}Cs concentrations (Table 4). Previous laboratory experiments with salmonids (Matsuda et al., 2020) and cyprinids (Wada et al., 2023) have demonstrated that dietary intake, rather than uptake from water, is the dominant pathway for ^{137}Cs accumulation in freshwater fish. Many aquatic insects and benthic foraging fish derive nutrition directly from sediment-associated materials (Pledger et al., 2014; Fenoglio et al., 2020), suggesting a more direct trophic linkage between sediment contamination and ^{137}Cs accumulation in fish than for water or soil. Taken together, these findings all suggest that the observed spatial differences in fish ^{137}Cs concentrations are most plausibly explained by localized dietary exposure shaped by site-specific food web structures. In this framework, ambient ^{137}Cs concentrations in the environment are considered to influence fish contamination levels indirectly, primarily by modulating the ^{137}Cs concentrations of their prey.

In the study region, fallout deposition patterns varied among river systems: deposition was highest in upstream sites of the Ukedo and Takase Rivers, whereas in the Kuma River, higher deposition occurred near the estuary than upstream (Fig. 1; Table S1). This variation allowed us to evaluate not only the effects of contamination level on ^{137}Cs concentrations in fish but also to assess the influence of land cover independently of contamination gradients by comparing across rivers with differing spatial patterns of fallout. Among the tested predictors, forest cover in the surrounding land use was the most effective variable for explaining fish ^{137}Cs concentrations (Table 4), outperforming environmental ^{137}Cs contamination levels. Given the relatively constant fish/prey concentration ratio across sites, the observed spatial variation in fish contamination likely reflects differences in ^{137}Cs accumulation by prey organisms rather than differences in trophic transfer efficiency. Stream fish are known to rely heavily on terrestrial insects as a food source, and forests tend to support higher fluxes of such prey than open landscapes, such as grasslands (Kawaguchi and Nakano, 2001; Grunblatt et al., 2019; Wada et al., 2024). Among terrestrial invertebrates, omnivorous, detritivorous, and fungivorous insects — especially those feeding on leaf litter and fungi — often exhibit elevated ^{137}Cs concentrations (Murakami et al., 2014; Ishii et al., 2017). Thus, fish in forested habitats may be exposed to greater ^{137}Cs through terrestrial trophic pathways due to a higher intake of these contaminated prey types. In addition to trophic factors, ionic competition between cesium and potassium can reduce ^{137}Cs uptake in freshwater fish (Rowan and Rasmussen, 1994; Wada et al., 2023). Upstream forested sites typically exhibit lower potassium concentrations than downstream areas affected by runoff and erosion (Ueda et al., 2013; Wada et al., 2023), potentially enhancing ^{137}Cs bioavailability.

4.2. Effects of migratory behavior on ^{137}Cs dynamics

Euryhaline fish species are known for tolerating a wide range of salinities and often migrate between freshwater and marine environments (Vij et al., 2020). In the present study, species-specific patterns in ^{137}Cs concentrations were observed, reflecting differences in their migratory behavior.

Masu salmon, an anadromous salmonid, varies in migratory forms, including sea-run and fluvial types (Morita, 2018). Sea-run individuals undergo hormonally regulated downstream migration, overwinter in the ocean, and return to rivers, while fluvial individuals remain in freshwater habitats throughout their life cycle (Munakata, 2012). In our study, masu salmon, primarily collected from upstream river sites, exhibited significantly higher ^{137}Cs concentrations than all other

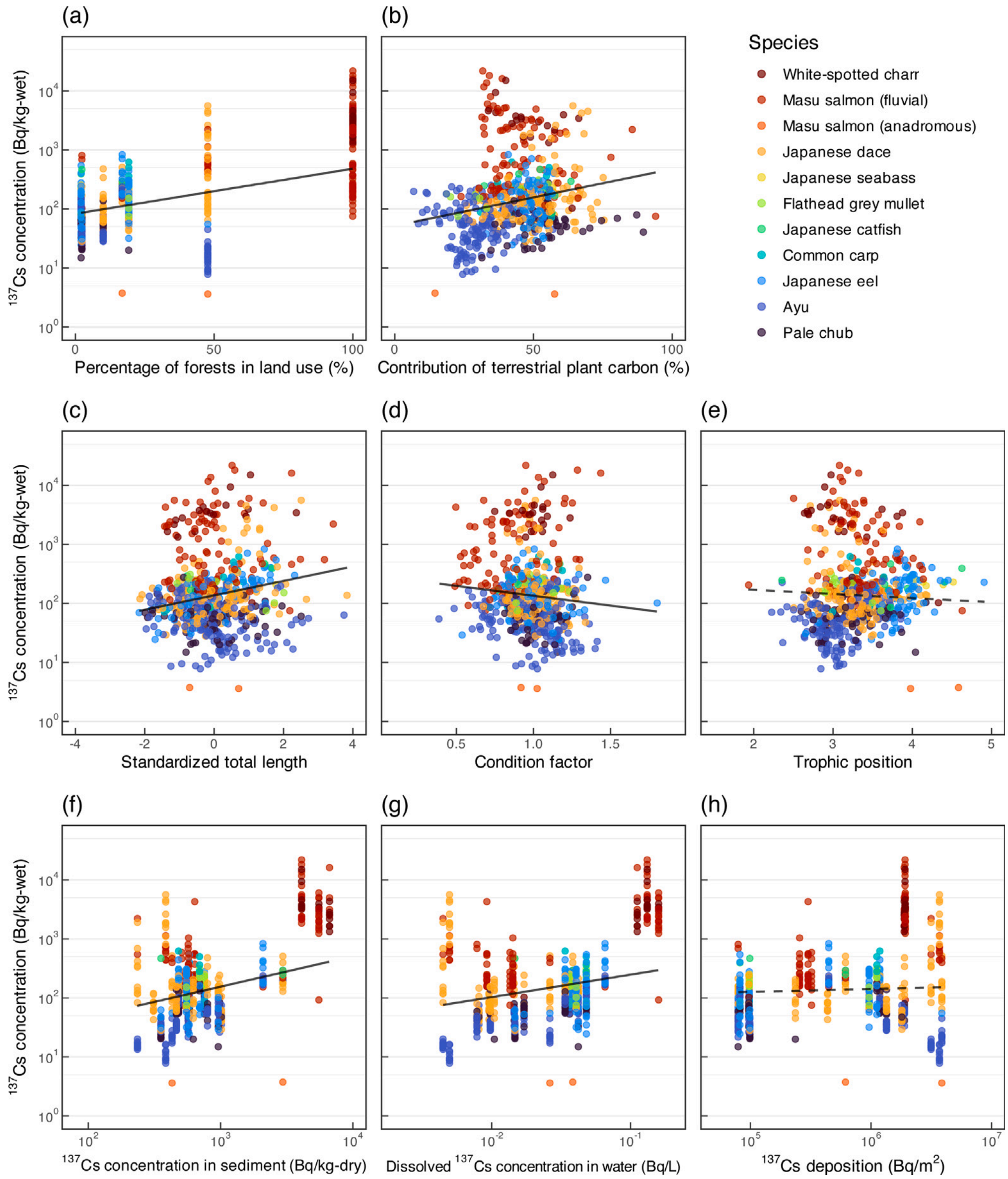

Fig. 5. Relationships between each explanatory variable and log-transformed ^{137}Cs concentrations in fish. Points are colored by species, and lines represent model-predicted values based on the best-supported generalized linear model (Table 4). Solid lines indicate statistically significant relationships ($p < 0.05$), while dashed lines indicate nonsignificant relationships ($p \geq 0.05$).

species except for white-spotted charr (Fig. 3). Nevertheless, two sea-run individuals collected from separate sites displayed much lower concentrations, approximately 4.0 Bq/kg-wet, markedly lower than the sympatric fluvial forms (Fig. 4a). The Ministry of Agriculture, Forestry and Fisheries (2025) published monitoring data showing that all the sea-run masu salmon caught off the coast of Fukushima between 2020 and 2022 had ^{137}Cs concentrations below detection limits (n = 2, < 8.0 Bq/kg-wet). Therefore, the ^{137}Cs levels observed in sea-run masu salmon in our study are consistent with oceanic values. This trend likely shows their limited feeding activity in freshwater following their return migration. A previous study reported a high proportion of empty stomachs in sea-run masu salmon captured in rivers, suggesting minimal feeding activity after upstream migration (Tago, 2000). Their low ^{137}Cs concentrations likely reflect limited intake of contaminated freshwater prey. This result underscores the importance of ecological traits — such as feeding behavior, habitat use, and migratory history — over species identity in determining ^{137}Cs accumulation. In species like masu salmon, which exhibit multiple migratory forms, such intraspecific variation can result in markedly different contamination levels.

Other euryhaline species investigated in this study include Japanese seabass and flathead grey mullet, which are marine amphidromous fish species. Although Japanese seabass generally inhabit coastal marine areas, some individuals migrate into freshwater, and juveniles in rivers benefit from abundant food, exhibiting rapid growth (Fuji et al., 2010; Kasai et al., 2018; Takai et al., 2024). Flathead grey mullet also utilize diverse aquatic habitats across their life history and demonstrate amphidromous migration (Chang et al., 2004; Whitfield et al., 2012). In the present study, Japanese seabass and flathead grey mullet collected from river sites showed ^{137}Cs concentrations comparable to or higher than those of typical freshwater fish at the exact locations (Fig. 4b). On the other hand, nearly all Japanese seabass samples (n = 262) from offshore Fukushima were below detection limits for ^{137}Cs (< 1.1×10 Bq/kg-wet), according to monitoring data published between 2020 and 2022 (Ministry of Agriculture, Forestry and Fisheries, 2025). All flathead grey mullet samples (n = 3) from offshore Fukushima were non-detectable (< 1.0×10 Bq/kg-wet), according to the data. These results suggest that the riverine individuals of these species actively consumed prey within the freshwater environment, thereby accumulating ^{137}Cs to levels similar to or greater than those of resident freshwater species. Such accumulation patterns due to feeding history are supported by previous findings from the Maeda River in Fukushima, where euryhaline fish exhibited similar ^{137}Cs concentrations after river migration (Wada et al., 2023).

4.3. Role of individual traits in explaining variability in ^{137}Cs concentrations

Fish/water concentration ratios of ^{137}Cs have been widely used as an indicator of radiocesium dynamics in aquatic ecosystems (Howard et al., 2013; Beresford et al., 2013; Wada et al., 2019, 2023; Ishii et al., 2020). In this study, the observed variation in concentration ratios among fish samples was considerable, ranging from 9.7×10 to 1.2×10^6 L/kg-wet, exceeding values reported in previous studies, and differing among species (Fig. 3). Laboratory experiments have shown that when multiple salmonid species are fed the same ^{137}Cs-labeled diet, their muscle ^{137}Cs concentrations reach similar steady-state levels, with no apparent interspecific difference (Matsuda and Yamamoto, 2025). These findings suggest that variation in ^{137}Cs concentrations among individual fish is primarily determined by the ^{137}Cs concentrations of ingested prey rather than by environmental water or physiological differences among species. Accordingly, species-level trends in ^{137}Cs accumulation likely reflect differences in dietary habits. Given the extensive variability in concentration ratios observed both across and within species, our results highlight the limited usefulness of concentration ratios as predictors of ^{137}Cs contamination in freshwater fish, and emphasize the need for alternative or improved indicators that incorporate dietary pathways and ecosystem-specific factors.

Stable isotope analysis revealed species-specific differences in carbon source contributions and trophic positions (Figs. S2, S3). For example, ayu, known for its firm reliance on algae (Ueda and Okada, 1934; Abe et al., 2006), showed significantly lower terrestrial carbon contributions than most other species (Fig. S2). Such interspecific variation likely reflects differences in feeding habits, prey availability from neighboring or upstream habitats, and interspecific competition. By quantitatively linking these individual-level dietary parameters to ^{137}Cs concentrations, this study moved beyond species-level generalizations to evaluate the role of individual traits. The proportion of terrestrial carbon in individual fish, estimated using carbon isotope signatures of terrestrial and aquatic primary producers at each site, was positively associated with fish ^{137}Cs concentrations and showed relatively strong explanatory power (Table 4; Fig. 5). In forested stream ecosystems, detrital pathways based on terrestrial leaf litter are known to serve as primary routes for ^{137}Cs transfer (Murakami et al., 2014), although primary producers such as periphyton may also play a role (Sakai et al., 2016). Fish feeding heavily on detritivorous terrestrial insects may thus occupy central positions in the ^{137}Cs-contaminated food web and be more directly exposed to terrestrial sources than those feeding mainly on aquatic producers.

While this study found a lower contribution of the periphyton-based food web to ^{137}Cs transfer to fish compared to terrestrial pathways, previous research conducted in mid-to-lower reaches of rivers reported that periphyton served as a major ^{137}Cs source for fish (Ishii et al., 2023). These discrepancies may reflect differences in river geomorphology and surrounding ecosystems; for instance, wider channels in downstream reaches can dilute the influence of terrestrial carbon inputs relative to in-stream primary production, leading to a greater reliance on periphyton-based pathways. Additional factors such as variation in target species or isotopic and chemical changes associated with decomposing leaf litter may also contribute to the contrasting patterns (Hall and Meyer, 1998; Sakai et al., 2016). Nevertheless, carbon stable isotope ratios were consistently selected as influential predictors of ^{137}Cs concentrations, highlighting multiple trophic pathways for ^{137}Cs transfer and their variable importance.

A well-known phenomenon in aquatic radioecology is the "size effect", wherein larger individuals tend to accumulate more radiocesium. Previous studies have linked this pattern to factors such as body length, weight, trophic position, and nutritional status. Key findings from freshwater fish studies include the following: (1) Positive correlations between body size (length or weight) and radiocesium concentrations have been widely reported across species and ecosystems (Koulikov and Ryabov, 1992; Ugedal et al., 1995; Brittain and Gjerseth, 2010; Wada et al., 2019, 2023, 2024). (2) In lakes and other semi-closed systems, radiocesium concentrations tend to increase with trophic level, resulting in higher concentrations in predatory fish (Hadderingh et al., 1997; Sundbom et al., 2003; Matsuda et al., 2015; Wada et al., 2019); in contrast, this pattern is less evident in rivers (Ishii et al., 2020, 2023). (3) Some studies have reported that radiocesium concentrations are more closely associated with condition factor — a proxy for nutritional status — than with size, suggesting that poorly nourished individuals may accumulate less ^{137}Cs (Ishii et al., 2021). Although these findings highlight several biological factors potentially contributing to the size effect, the underlying mechanisms remain poorly understood, especially in riverine ecosystems.

In our study, we assessed the size effect at the individual level, independent of species identity, by modeling the effects of standardized body length, condition factor, and trophic position across 10 riverine fish species. Standardized length was positively associated with ^{137}Cs concentrations and had relatively strong explanatory power, while condition factor and trophic position showed weak negative associations (Table 4; Fig. 5). These results are consistent with previously reported size-^{137}Cs relationships (1 and 2), and the weak, nonsignificant effect of condition factor suggests a limited role of nutritional status (3) under the riverine conditions of this study. To interpret the underlying mechanisms of this size effect, it is informative to compare riverine systems with lakes, where piscivory is more common and size-^{137}Cs relationships are often stronger. Stomach content analyses have indicated that piscivory tends to be more prevalent in lakes, whereas insectivory dominates in riverine fish communities (Yoshimura and Yokoduka, 2014; Wada et al., 2024). In lakes, piscivory has been associated with elevated ^{137}Cs concentrations, and larger individuals may accumulate more due to ontogenetic dietary shifts toward predation (Ishii et al., 2020). This trend likely reflects ecosystem-specific food web structures, where fish-based diets contribute more substantially to ^{137}Cs accumulation than detritus- or algae-based diets. In contrast, piscivory is less common in riverine fish, and the link between body size, trophic position, and ^{137}Cs concentration appears weaker. In such systems, non-dietary mechanisms may play a significant role. Laboratory studies suggest that age-related declines in metabolic and excretion rates may enhance ^{137}Cs retention in older individuals (Ugedal et al., 1992; Matsuda and Yamamoto, 2025), potentially contributing to the observed size effect. Larger, older fish may retain ^{137}Cs for more extended periods due to slower physiological turnover (Kryshev and Ryabov, 2000).

5. Conclusion

This study analyzed spatial and interspecific variation in ^{137}Cs concentrations among ten freshwater fish species collected from upstream to downstream reaches of multiple river systems affected by radiocesium fallout from the FDNPP accident. The results demonstrated that ^{137}Cs concentrations varied depending on the sampling site, species identity, and migratory behavior. Analysis of individual-level predictors revealed that fish captured in forested areas tended to have higher ^{137}Cs concentrations, and individuals with greater contributions from terrestrial carbon sources, as estimated by stable isotope analysis, also exhibited elevated levels of contamination. A general size effect was observed, whereby larger individuals accumulated more ^{137}Cs, consistent with previous findings in freshwater ecosystems.

These findings contribute to both species- and site-specific understanding of radiocesium dynamics and the development of more generalizable predictors of contamination that account for individual-level variability. They also emphasize the importance of food-web perspectives in evaluating radiocesium accumulation beyond species identity alone. In particular, dietary history, habitat use, and migratory traits emerged as key factors shaping contamination levels within and across species.

To advance predictive understanding, future research should integrate seasonal datasets, include isotopic and radiocesium measurements of prey organisms, and examine broader habitat gradients, including estuarine and marine phases of migratory species. Further investigations are also needed to clarify how water chemistry parameters other than potassium concentrations influence ^{137}Cs bioavailability, and to elucidate the mechanisms that can generate extremely high concentration ratios. Future research could also improve upon conventional concentration ratios by incorporating variables that showed strong explanatory power in our models, such as ^{137}Cs concentrations in sediment and forest cover, thereby developing alternative indices more closely tied to ecological processes. Such efforts will improve the robustness of ecological models and inform long-term risk assessment and management of freshwater fish contamination in post-nuclear landscapes. Our findings offer a scientific basis for monitoring strategies and ecosystem restoration planning in affected watersheds.

CRediT authorship contribution statement

Minato Kakuma: Writing – review & editing, Writing – original draft, Visualization, Methodology, Investigation, Funding acquisition, Conceptualization. **Toshihiro Wada:** Writing – review & editing, Resources, Methodology, Investigation, Funding acquisition, Conceptualization. **Masashi Murakami:** Writing – review & editing, Supervision, Investigation, Conceptualization. **Takahiro Tatsuno:** Resources, Investigation. **Nobuyoshi Ishii:** Resources, Investigation, Conceptualization. **Natsuko I. Kobayashi:** Resources, Investigation. **Takumi Kurosawa:** Investigation, Data curation. **Yo Sayama:** Visualization, Investigation. **Naoto Nihei:** Investigation, Conceptualization. **Nobuhito Ohte:** Writing – review & editing, Supervision, Project administration, Investigation, Funding acquisition, Conceptualization.

Declaration of Generative AI and AI-assisted technologies in the writing process

During the preparation of this work, the authors used ChatGPT (OpenAI) in order to improve the clarity, grammar, and structure of the English text, and to refine scientific expressions based on journal guidelines. After using this tool, the authors reviewed and edited the content as needed and take full responsibility for the content of the publication.

Declaration of competing interest

The authors declare that they have no known competing financial interests or personal relationships that could have appeared to influence the work reported in this paper.

Acknowledgments

This work was supported by the Japan Society for the Promotion of Science (JSPS) through a Grant-in-Aid for JSPS Fellows (JP22KJ1930) and a JSPS KAKENHI Grant (JP20H00435), as well as by the Fukushima Institute for Research, Education and Innovation (F-REI) through a commissioned research fund (JPFR25050501). The authors thank Honoka Kurosawa and Hiromichi Waki for their valuable assistance with sample processing and analysis.

Appendix A. Supplementary data

Supplementary material related to this article can be found online at https://doi.org/10.1016/j.jenvrad.2025.107810.

Data availability

Data will be made available on request.

References

Abe, S.I., Kiso, K., Katano, O., Yamamoto, S., Nagumo, T., Tanaka, J., 2006. Impacts of differential consumption by the grazing fish, *Plecoglossus altivelis*, on the benthic algal composition in the chikuma river, Japan. Phycol. Res. 54 (2), 94–98. http://dx.doi.org/10.1111/j.1440-1835.2006.00413.x.

Aoyama, M., Inomata, Y., Tsumune, D., Tateda, Y., 2019. Fukushima radionuclides in the marine environment from coastal region of Japan to the Pacific ocean through the end of 2016. Prog. Nucl. Sci. Technol. 6, 1–7. http://dx.doi.org/10.15669/pnst.6.1.

Bartoń, K., 2023. MuMIn: Multi-model inference. URL https://CRAN.R-project.org/package=MuMIn.

Bates, D., Mächler, M., Bolker, B., Walker, S., 2015. Fitting linear mixed-effects models using lme4. J. Stat. Softw. 67 (1), 1–48. http://dx.doi.org/10.18637/jss.v067.i01.

Beresford, N.A., Yankovich, T.L., Wood, M.D., Fesenko, S., Andersson, P., Muikku, M., Willey, N.J., 2013. A new approach to predicting environmental transfer of radionuclides to wildlife: a demonstration for freshwater fish and caesium. Sci. Total Environ. 463–464, 284–292. http://dx.doi.org/10.1016/j.scitotenv.2013.06.013.

Brittain, J., Gjerseth, J., 2010. Long-term trends and variation in ^{137}Cs activity concentrations in brown trout (*Salmo trutta*) from Øvre Heimdalsvatn, a norwegian subalpine lake. In: Brittain, J., Borgstrø m, R. (Eds.), The Subalpine Lake Ecosystem, Øvre Heimdalsvatn, and Its Catchment: Local and Global Changes over the Last 50 Years. Springer, Dordrecht, pp. 107–113. http://dx.doi.org/10.1007/s10750-010-0155-5.

Caut, S., Angulo, E., Courchamp, F., 2009. Variation in discrimination factors (δ^{15}N and δ^{13}C): the effect of diet isotopic values and applications for diet reconstruction. J. Appl. Ecol. 46 (2), 443–453. http://dx.doi.org/10.1111/j.1365-2664.2009.01620.x.

Chang, C.W., Iizuka, Y., Tzeng, W.N., 2004. Migratory environmental history of the grey mullet mugil cephalus as revealed by otolith Sr:Ca ratios. Mar. Ecol. Prog. Ser. 269, 277–288. http://dx.doi.org/10.3354/meps269277.

Fenoglio, S., Tierno de Figueroa, J.M., Doretto, A., Falasco, E., Bona, F., 2020. Aquatic insects and benthic diatoms: A history of biotic relationships in freshwater ecosystems. Water (Basel) 12 (10), 2934. http://dx.doi.org/10.3390/w12102934.

Fox, J., Weisberg, S., 2019. Car: Companion to applied regression. URL https://socialsciences.mcmaster.ca/jfox/Books/Companion/.

Fuji, T., Kasai, A., Suzuki, K.W., Ueno, M., Yamashita, Y., 2010. Freshwater migration and feeding habits of juvenile temperate seabass *Lateolabrax japonicus* in the stratified Yura River estuary, the Sea of Japan. Fish. Sci. 76 (4), 643–652. http://dx.doi.org/10.1007/s12562-010-0258-y.

Fukushima Prefecture, 2024. Transition of the evacuation zones -Explanation-. URL https://www.pref.fukushima.lg.jp/site/portal-english/en-1-3-1.html. (Accessed 15 December 2024).

Grunblatt, J., Meyer, B.E., Wipfli, M.S., 2019. Invertebrate prey contributions to juvenile Coho Salmon diet from riparian habitats along three Alaska streams: Implications for environmental change. J. Freshw. Ecol. 34 (1), 617–631. http://dx.doi.org/10.1080/02705060.2019.1642243.

Hadderingh, R.H., van Aerssen, G.H.F.M., Ryabov, I.N., Koulikov, A.O., Belova, N., 1997. Contamination offish with ^{137}Cs in Kiev reservoir and old river bed of Pripyat near Chernobyl. Stud. Env. Sci. 68, 339–351. http://dx.doi.org/10.1016/S0166-1116(09)70113-X.

Hall, Jr., R.O., Meyer, J.L., 1998. The trophic significance of bacteria in a detritus-based stream food web. Ecology 79 (6), 1995–2012. http://dx.doi.org/10.1890/0012-9658(1998)079[1995:TTSOBI]2.0.CO;2.

Haque, M.E., Gomi, T., Sakai, M., Negishi, J.N., 2017. Developing a food web-based transfer factor of radiocesium for fish, whitespotted char (*Salvelinus leucomaenis*) in headwater streams. J. Environ. Radioact. 172, 191–200. http://dx.doi.org/10.1016/j.jenvrad.2017.02.020.

Hayashi, S., 2016. Migration and accumulation of radioactive cesium in the upstream region of river watersheds affected by the Fukushima Daiichi Nuclear Power Plant accident: a review. Glob Env. Res 20, 45–52, URL https://airies.wikiplus.net/journal_20-1-2eng.html. (Accessed 12 June 2025).

Howard, B.J., Beresford, N.A., Copplestone, D., Telleria, D., Proehl, G., Fesenko, S., Jeffree, R.A., Yankovich, T.L., Brown, J.E., Higley, K., Johansen, M.P., Mulye, H., Vandenhove, H., Gashchak, S., Wood, M.D., Takata, H., Andersson, P., Dale, P., Ryan, J., Bollhöfer, A., Doering, C., Barnett, C.L., Wells, C., 2013. The IAEA handbook on radionuclide transfer to wildlife. J. Environ. Radioact. 121, 55–74. http://dx.doi.org/10.1016/j.jenvrad.2012.01.027.

Ishii, N., Furota, T., Kagami, M., Tagami, K., Uchida, S., 2021. Inequality in the distribution of ^{137}Cs contamination within freshwater fish bodies and its affecting factors. Sci. Rep. 11 (1), 5769. http://dx.doi.org/10.1038/s41598-021-85291-6.

Ishii, Y., Hayashi, S., Takamura, N., 2017. Radiocesium transfer in forest insect communities after the Fukushima Dai-ichi Nuclear Power Plant accident. PLoS One 12 (1), e0171133. http://dx.doi.org/10.1371/journal.pone.0171133.

Ishii, Y., Matsuzaki, S.I.S., Hayashi, S., 2020. Different factors determine ^{137}Cs concentration factors of freshwater fish and aquatic organisms in lake and river ecosystems. J. Environ. Radioact. 213, 106102. http://dx.doi.org/10.1016/j.jenvrad.2019.106102.

Ishii, Y., Nakagawa, M., Matsuzaki, S.I.S., Jo, J., Hayashi, S., 2023. Contrasting radiocesium transfer in the river and lake food webs: Importance of trophic level and food source. J. Environ. Radioact. 263, 107184. http://dx.doi.org/10.1016/j.jenvrad.2023.107184.

Japan Aerospace Exploration Agency, 2023. High-resolution land-use and land-cover map of Japan. URL https://www.eorc.jaxa.jp/ALOS/en/dataset/lulc/lulc_v2312_e.htm. (Accessed 10 December 2024).

Japan Atomic Energy Agency, 2024. Database for radioactive substance monitoring data/GSI maps. URL https://emdb.jaea.go.jp/emdb/top. (Accessed 15 December 2024).

Kasai, A., Fuji, T., Suzuki, K.W., Yamashita, Y., 2018. Partial migration of juvenile temperate seabass *Lateolabrax japonicus*: a versatile survival strategy. Fish. Sci. 84 (2), 153–162. http://dx.doi.org/10.1007/s12562-017-1166-1.

Kawaguchi, Y., Nakano, S., 2001. Contribution of terrestrial invertebrates to the annual resource budget for salmonids in forest and grassland reaches of a headwater stream. Freshw. Biol. 46 (3), 303–316. http://dx.doi.org/10.1046/j.1365-2427.2001.00667.x.

Koulikov, A.O., Ryabov, I.N., 1992. Specific cesium activity in freshwater fish and the size effect. Sci. Total Environ. 112 (1), 125–142. http://dx.doi.org/10.1016/0048-9697(92)90243-L.

Kryshev, A.I., Ryabov, I.N., 2000. A dynamic model of ^{137}Cs accumulation by fish of different age classes. J. Environ. Radioact. 50 (3), 221–233. http://dx.doi.org/10.1016/S0265-931X(99)00118-6.

Kurikami, H., Sakuma, K., Malins, A., Sasaki, Y., Niizato, T., 2019. Numerical study of transport pathways of ^{137}Cs from forests to freshwater fish living in mountain streams in Fukushima, Japan. J. Environ. Radioact. 208–209, 106005. http://dx.doi.org/10.1016/j.jenvrad.2019.106005.

Matsuda, K., Takagi, K., Tomiya, A., Enomoto, M., Tsuboi, J.I., Kaeriyama, H., Ambe, D., Fujimoto, K., Ono, T., Uchida, K., Morita, T., Yamamoto, S., 2015. Comparison of radioactive cesium contamination of lake water, bottom sediment, plankton, and freshwater fish among lakes of Fukushima Prefecture, Japan after the Fukushima fallout. Fish. Sci. 81 (4), 737–747. http://dx.doi.org/10.1007/s12562-015-0874-7.

Matsuda, K., Yamamoto, S., 2025. Influence of body size on the uptake or depuration of ^{137}Cs originating from feed in three salmonid species. Fish. Sci. 91, 89–98. http://dx.doi.org/10.1007/s12562-024-01840-8.

Matsuda, K., Yamamoto, S., Miyamoto, K., 2020. Comparison of ^{137}Cs uptake, depuration and continuous uptake, originating from feed, in five salmonid fish species. J. Environ. Radioact. 222, 106350. http://dx.doi.org/10.1016/j.jenvrad.2020.106350.

Ministry of Agriculture, Forestry and Fisheries, 2025. Results of the monitoring on radioactivity level in fishery products. URL https://www.jfa.maff.go.jp/e/inspection/index.html. (Accessed 15 May 2025).

Morita, K., 2018. General biology of masu salmon. In: Beamish, R.J. (Ed.), The Ocean Ecology of Pacific Salmon and Trout. American Fisheries Society, Bethesda, pp. 703–730.

Munakata, A., 2012. Migratory behaviors in masu salmon (*Oncorhynchus masou*) and the influence of endocrinological factors. Aqua-BioScience Monogr. 5 (2), 29–65. http://dx.doi.org/10.5047/absm.2012.00502.0029.

Murakami, M., Ohte, N., Suzuki, T., Ishii, N., Igarashi, Y., Tanoi, K., 2014. Biological proliferation of cesium-137 through the detrital food chain in a forest ecosystem in Japan. Sci. Rep. 4 (1), 3599. http://dx.doi.org/10.1038/srep03599.

Nakanishi, T., Sakuma, K., 2019. Trend of ^{137}Cs concentration in river water in the medium term and future following the Fukushima nuclear accident. Chemosphere 215, 272–279. http://dx.doi.org/10.1016/j.chemosphere.2018.10.017.

Ohte, N., Murakami, M., Endo, I., Ohashi, M., Iseda, K., Suzuki, T., Oda, T., Hotta, N., Tanoi, K., Kobayashi, N.I., Ishii, N., 2016. Ecosystem monitoring of radiocesium redistribution dynamics in a forested catchment in Fukushima after the nuclear power plant accident in March 2011. In: Nakanishi, T.M., Tanoi, K. (Eds.), Agricultural Implications of the Fukushima Nuclear Accident. Springer, Tokyo, pp. 175–188. http://dx.doi.org/10.1007/978-4-431-55828-6_14.

Pledger, A.G., Rice, S.P., Millett, J., 2014. Reduced bed material stability and increased bedload transport caused by foraging fish: a flume study with juvenile Barbel (*Barbus barbus*). Earth Surf. Process. 39 (11), 1500–1513. http://dx.doi.org/10.1002/esp.3592.

Plummer, M., 2024. Rjags: Bayesian graphical models using MCMC. URL https://CRAN.R-project.org/package=rjags.

Post, D.M., 2002. Using stable isotopes to estimate trophic position: models, methods, and assumptions. Ecology 83 (3), 703–718. http://dx.doi.org/10.1890/0012-9658(2002)083[0703:USITET]2.0.CO;2.

Post, D.M., Layman, C.A., Arrington, D.A., Takimoto, G., Quattrochi, J., Montaña, C.G., 2007. Getting to the fat of the matter: models, methods and assumptions for dealing with lipids in stable isotope analyses. Oecologia 152 (1), 179–189. http://dx.doi.org/10.1007/s00442-006-0630-x.

QGIS Development Team, 2024. QGIS. URL https://www.qgis.org/.

R. Core Team, 2024. R: A language and environment for statistical computing. URL https://www.R-project.org/.

Rowan, D.J., Rasmussen, J.B., 1994. Bioaccumulation of radiocesium by fish: The influence of physicochemical factors and trophic structure. Can. J. Fish. Aquat. Sci. 51 (11), 2388–2410. http://dx.doi.org/10.1139/f94-240.

Sakai, M., Gomi, T., Negishi, J.N., Iwamoto, A., Okada, K., 2016. Different cesium-137 transfers to forest and stream ecosystems. Environ. Pollut. 209, 46–52. http://dx.doi.org/10.1016/j.envpol.2015.11.025.

Sakai, M., Tsuji, H., Ishii, Y., Ozaki, H., Takechi, S., Jo, J., Tamaoki, M., Hayashi, S., Gomi, T., 2021. Untangling radiocesium dynamics of forest-stream ecosystems: A review of fukushima studies in the decade after the accident. Environ. Pollut. 288, 117744. http://dx.doi.org/10.1016/j.envpol.2021.117744.

Schneider, G., Chicken, E., Becvarik, R., 2023. NSM3: Functions and datasets to accompany hollander, Wolfe, and Chicken - nonparametric statistical methods, third edition. URL https://CRAN.R-project.org/package=NSM3.

Stock, B.C., Jackson, A.L., Ward, E.J., Parnell, A.C., Phillips, D.L., Semmens, B.X., 2018. Analyzing mixing systems using a new generation of Bayesian tracer mixing models. PeerJ 6, e5096. http://dx.doi.org/10.7717/peerj.5096.

Sundbom, M., Meili, M., Andersson, E., Östlund, M., Broberg, A., 2003. Long-term dynamics of Chernobyl ^{137}Cs in freshwater fish: quantifying the effect of body size and trophic level: Long-term dynamics of chernobyl ^{137}Cs in fish. J. Appl. Ecol. 40 (2), 228–240. http://dx.doi.org/10.1046/j.1365-2664.2003.00795.x.

Tago, Y., 2000. Upstream migration and summer stay of adult masu salmon in the Jinzu and Shou rivers of the Hokuriku region. Nippon. Suisan Gakkai Shi 66 (1), 44–49. http://dx.doi.org/10.2331/suisan.66.44, [in Japanese with English abstract].

Takai, K., Kuroki, M., Shirai, K., Manabu, K., Murakami, H., Terashima, Y., Mitamura, H., Yamashita, Y., 2024. River-sea migration patterns of juvenile Japanese seabass influence migrations in subsequent stages. Estuar. Coast. Shelf Sci. 307, 108921. http://dx.doi.org/10.1016/j.ecss.2024.108921.

Tsuji, H., Kondo, Y., Suzuki, Y., Yasutaka, T., 2014a. Development of a method for rapid and simultaneous monitoring of particulate and dissolved radiocesium in water with nonwoven fabric cartridge filters. J. Radioanal. Nucl. Chem. 299 (1), 139–147. http://dx.doi.org/10.1007/s10967-013-2735-0.

Tsuji, H., Yasutaka, T., Kawabe, Y., Onishi, T., Komai, T., 2014b. Distribution of dissolved and particulate radiocesium concentrations along rivers and the relations between radiocesium concentration and deposition after the nuclear power plant accident in Fukushima. Water Res. 60, 15–27. http://dx.doi.org/10.1016/j.watres.2014.04.024.

Ueda, S., Hasegawa, H., Kakiuchi, H., Akata, N., Ohtsuka, Y., Hisamatsu, S., 2013. Fluvial discharges of radiocaesium from watersheds contaminated by the Fukushima Dai-ichi Nuclear Power Plant accident, Japan. J. Environ. Radioact. 118, 96–104. http://dx.doi.org/10.1016/j.jenvrad.2012.11.009.

Ueda, S., Okada, Y., 1934. On the food of the salmonoid fish, Ayu (*Plecoglossus altivelis* Temmninck & Schlegel). Nippon. Suisan Gakkai Shi 5 (2), 241–245. http://dx.doi.org/10.2331/suisan.2.241, [in Japanese with English abstract].

Ugedal, O., Forseth, T., Jonsson, B., Njastad, O., 1995. Sources of variation in radiocaesium levels between individual fish from a Chernobyl contaminated Norwegian lake. J. Appl. Ecol. 32 (2), 352. http://dx.doi.org/10.2307/2405101.

Ugedal, O., Jonsson, B., Nj˚ astad, O., Næ umann, R.f., 1992. Effects of temperature and body size on radiocaesium retention in brown trout, *Salmo trutta*. Freshw. Biol. 28 (2), 165–171. http://dx.doi.org/10.1111/j.1365-2427.1992.tb00573.x.

Vij, S., Purushothaman, K., Sridatta, P., Jerry, D., 2020. Transcriptomic analysis of gill and kidney from Asian seabass (*Lates calcarifer*) acclimated to different salinities reveals pathways involved with euryhalinity. Genes (Basel) 11 (7), 733. http://dx.doi.org/10.3390/genes11070733.

Wada, T., Hinata, A., Furuta, Y., Sasaki, K., Konoplev, A., Nanba, K., 2023. Factors affecting ^{137}Cs radioactivity and water-to-body concentration ratios of fish in river and pond environments near the Fukushima Dai-ichi Nuclear Power Plant. J. Environ. Radioact. 258, 107103. http://dx.doi.org/10.1016/j.jenvrad.2022.107103.

Wada, T., Konoplev, A., Wakiyama, Y., Watanabe, K., Furuta, Y., Morishita, D., Kawata, G., Nanba, K., 2019. Strong contrast of cesium radioactivity between marine and freshwater fish in Fukushima. J. Environ. Radioact. 204, 132–142. http://dx.doi.org/10.1016/j.jenvrad.2019.04.006.

Wada, T., Nemoto, Y., Fujita, T., Kawata, G., Kamiyama, K., Sohtome, T., Narita, K., Watanabe, M., Shimamura, S., Enomoto, M., Suzuki, S., Amano, Y., Morishita, D., Matsumoto, A., Morioka, Y., Tomiya, A., Sato, T., Niizeki, K., Iwasaki, T., Sato, M., Mizuno, T., Nanba, K., 2022. Cesium radioactivity in marine and freshwater products and its relation to the restoration of fisheries in Fukushima: A decade review. In: Nanba, K., Konoplev, A., Wada, T. (Eds.), Behavior of Radionuclides in the Environment III. Springer, Singapore, pp. 313–351. http://dx.doi.org/10.1007/978-981-16-6799-2_14.

Wada, T., Suzuki, S., Kanasashi, T., Nanba, K., 2024. Distinct food-web transfers of ^{137}Cs to fish in river and lake ecosystems: A case study focusing on masu salmon in the Fukushima evacuation zone. J. Environ. Radioact. 280, 107541. http://dx.doi.org/10.1016/j.jenvrad.2024.107541.

Wada, T., Tomiya, A., Enomoto, M., Sato, T., Morishita, D., Izumi, S., Niizeki, K., Suzuki, S., Morita, T., Kawata, G., 2016. Radiological impact of the nuclear power plant accident on freshwater fish in Fukushima: An overview of monitoring results. J. Environ. Radioact. 151 (1), 144–155. http://dx.doi.org/10.1016/j.jenvrad.2015.09.017.

Whitfield, A.K., Panfili, J., Durand, J.-D., 2012. A global review of the cosmopolitan flathead mullet *Mugil cephalus* linnaeus 1758 (teleostei: Mugilidae), with emphasis on the biology, genetics, ecology and fisheries aspects of this apparent species complex. Rev. Fish Biol. Fish. 22 (3), 641–681. http://dx.doi.org/10.1007/s11160-012-9263-9.

Yamamoto, S., Mutou, K., Nakamura, H., Miyamoto, K., Uchida, K., Takagi, K., Fujimoto, K., Kaeriyama, H., Ono, T., 2015. Assessment of radiocesium accumulation by hatchery-reared salmonids after the fukushima nuclear accident. In: Nakata, K., Sugisaki, H. (Eds.), Impacts of the Fukushima Nuclear Accident on Fish and Fishing Grounds. Springer, Tokyo, pp. 231–238. http://dx.doi.org/10.1007/978-4-431-55537-7_19.

Yasutaka, T., Tsuji, H., Kondo, Y., Suzuki, Y., Takahashi, A., Kawamoto, T., 2015. Rapid quantification of radiocesium dissolved in water by using nonwoven fabric cartridge filters impregnated with potassium zinc ferrocyanide. J. Nucl. Sci. Technol. 52 (6), 792–800. http://dx.doi.org/10.1080/00223131.2015.1013071.

Yoshimura, M., Yokoduka, T., 2014. Radioactive contamination of fishes in lake and streams impacted by the Fukushima nuclear power plant accident. Sci. Total Environ. 482–483, 184–192. http://dx.doi.org/10.1016/j.scitotenv.2014.02.118.

Zuur, A.F., Ieno, E.N., Elphick, C.S., 2010. A protocol for data exploration to avoid common statistical problems: Data exploration. Methods Ecol. Evol. 1 (1), 3–14. http://dx.doi.org/10.1111/j.2041-210X.2009.00001.x.